

Study of design parameters on flutter stability of cable-stayed bridges

Xin-Jun Zhang[†]

Department of Civil Engineering, Zhejiang University of Technology, Hangzhou 310032, China

Bing-Nan Sun[‡]

Department of Civil Engineering, Zhejiang University, Hangzhou 310027, China

(Received January 1, 2003, Accepted August 9, 2003)

Abstract. Flutter stability is one of major concerns on the design of long-span cable-stayed bridges. Considering the geometric nonlinearity of cable-stayed bridges and the effects due to the nonlinear wind-structure interactions, a nonlinear method is proposed to analyze the flutter stability of cable-stayed bridges, and a computer program NFAB is also developed. Taking the Jingsha bridge over the Yangtze River as example, parametric analyses on flutter stability of the bridge are carried out, and some important design parameters that affect the flutter stability of cable-stayed bridges are pointed out.

Keywords: cable-stayed bridge; design parameters; flutter stability; nonlinear flutter analysis.

1. Instruction

Modern cable-stayed bridges, which were introduced in the mid 1950s and have been rapidly developed over the recent 30 years, are becoming very popular all over the world. The progress can be mainly owed to the development in the fields of computer technology, high strength steel cables, orthotropic steel deck and construction technology. Today, the cable-stayed bridge is considered as the most suitable solution for highway bridges with spans ranging from 200 m to about 1000 m because of its aesthetic appeal, economic grounds and ease of erection. Currently, the world's longest cable-stayed bridge is the Tatara bridge in Japan with a central span of 890 m. In recent years, many projects crossing the straits are being planned around the world, and a lot of long-span especially super long-span cable-stayed bridges or suspension bridges are proposed in these engineering projects. The increase in span length combined with the trend to more shallow or slender stiffening girders in cable-stayed bridges has raised concern about their behaviors under both service and environmental dynamic loadings such as traffic, wind and earthquake loadings. Among them, the wind stability is one of the major concerns for the designers. Generally, there are two important types of the wind instability for cable-stayed bridges including the aerostatic instabilities due to the static wind action and the aerodynamic instability due to the dynamic wind actions. The

[†] Associate Professor

[‡] Professor

flutter instability is the most important type of the aerodynamic instability, whereas the torsional divergence and the lateral buckling are the main types of aerostatic instability. However, the critical wind speed of flutter stability is generally less than that of aerostatic stability, and therefore as far as the wind stability is concerned, the flutter stability plays an important role in the wind-resistant design of cable-stayed bridges.

Comprehensive investigations have been made on the static behavior of cable-stayed bridges under the dead loads, traffic and static wind loading. The effects of some design parameters on the static characteristics such as the ratios of side span to main span and the tower's height to main span length, the tower's lateral configuration, and the subsidiary piers in side spans etc have been investigated. Besides the static characteristics, the dynamic characteristics and further the flutter stability are both inevitably affected by these parameters. But until now, few investigations have been made concerning the influence of these parameters on flutter stability of cable-stayed bridges, and the roles of these effects in flutter stability need to be further investigated.

In previous flutter analysis, the linear method is usually used, which is based on the undeformed initial structural configuration in wind flow, the geometric nonlinearity of bridge structures and the effects due to the nonlinear wind-structure interaction are neglected (Agar 1989, Scanlan and Jones 1990, Jain *et al.* 1996, Namini 1992, Ge and Tanaka 2000, Tanaka *et al.* 1992). But for long-span cable-stayed bridge, they will be greatly deformed under the static wind action due to their great flexibility. The large deformation, on the one hand, will affect structural stiffness and further the dynamic characteristics. On the other hand, the aerodynamic shape of deck section will be remarkably changed, which leads to the significant variation and non-uniform distribution of the wind forces acting on the bridge (Boonyapinyo *et al.* 1994, Chen *et al.* 2002, Zhang *et al.* 2000 and 2002). These effects will finally affect the aerodynamic response of the bridge under the dynamic wind action. Therefore, flutter analysis should be performed on the deformed structure under the static wind action to consider these effects.

In this paper, a method of three-dimensional nonlinear flutter analysis is presented, and a computer program NFAB is also developed. Taking the Jingsha bridge over the Yangtze River as example, parametric analyses on flutter stability of the bridge are carried out by NFAB, and some important design parameters that affect the flutter stability of cable-stayed bridges are pointed out.

2. Method of nonlinear flutter analysis

For long-span cable-stayed bridges, the geometric nonlinearity is strong due to the large deformation, cable sag and beam-column effects under the wind loading. In addition, the aerostatic and aerodynamic forces, which are two important types of the wind forces acting on the bridges, are displacement-dependent and the wind-structure interaction is nonlinear. Therefore, flutter analysis should be based on the equilibrium position under the static wind action. In general, flutter analysis is to find out the critical condition of flutter stability by gradually increasing the wind speed. In order to consider the effects due to the nonlinear wind-structure interaction, at every wind speed increment, the following two steps will be performed: (1) nonlinear aerostatic analysis to predicate the deformed equilibrium position under the static wind action; (2) aerodynamic response analysis on the deformed bridge structures under the static wind action to predicate the dynamic response under the dynamic wind action.

2.1. Three-dimensional nonlinear aerostatic analysis

The aerostatic effect is usually treated as an action of 3 aerostatic components of wind forces on bridge structures, namely the drag force F_z , lift force F_y and twist moment M_x , as shown in Fig. 1. However, the aerostatic forces change with the deformation of bridge structures and can be described as a function of the effective attack angle α_e between the wind flow and deformed bridge deck as shown in Fig. 1, which is the sum of initial wind attack angle θ_0 and the torsional angle θ caused by the static wind action. Meanwhile, the torsional angles vary along the bridge axis, and therefore the aerostatic forces are distributed un-uniformly along the bridge axis.

The static equilibrium equation of structural system under the static wind action can be expressed as:

$$[K(u)]\{u\} = P(F_y(\alpha_e), F_z(\alpha_e), M(\alpha_e)) \tag{1}$$

where $[K(u)]$ is the nonlinear stiffness matrix including elastic stiffness matrix and geometric stiffness matrix; $\{u\}$ is the nodal displacement vector; $P(F_y(\alpha_e), F_z(\alpha_e), M(\alpha_e))$ is the static wind load.

At a given wind speed U , Eq. (1) can be solved by the iteration method due to the non-linearities of both the bridge structure and the aerostatic forces. The procedure of determining the equilibrium position of the bridge under the static wind action can be summarized as follows:

1. Calculate the aerostatic load $\{F_0\}$ at the initial wind attack angles, let $\{F_2\}=\{F_0\}, \{F_1\}=\{0\}$.
2. Calculate the aerostatic load increment $\{\Delta F\}=\{F_2\}-\{F_1\}$, let $\{F_1\}=\{F_2\}$.
3. Predicate the deformed position under the incremental aerostatic load by three-dimensional geometric nonlinear analysis.
4. Determine the effective wind attack angle of the deck, and recalculate the aerostatic load $\{F_2\}$.
5. Check if the Euclidean norm of aerostatic coefficients is less than the prescribed tolerance. The Euclidean norm is expressed as (Boonyapinyo *et al.* 1994):

$$\left\{ \frac{\sum_1^{N_a} [C_K(\alpha_j) - C_K(\alpha_{j-1})]^2}{\sum_1^{N_a} [C_K(\alpha_{j-1})]^2} \right\}^{\frac{1}{2}} \leq \varepsilon_K \quad (K \text{ represents } L, D, M) \tag{2}$$

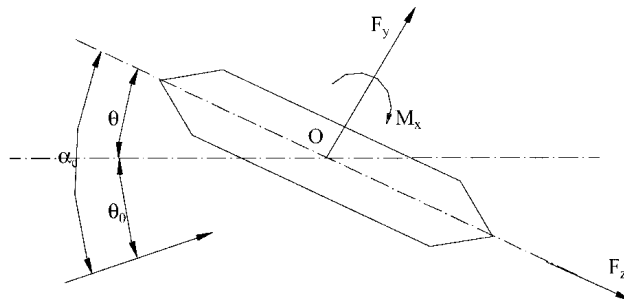


Fig. 1 The effective attack angle

$$[A_d]^e = \begin{bmatrix} 0 & 0 & 0 & 0 & 0 & 0 & 0 & 0 & 0 & 0 \\ 0 & BLKH_1^* & BLKH_5^* & -B^2LKH_2^* & 0 & 0 & 0 & 0 & 0 & 0 \\ 0 & BLKP_5^* & BLKP_1^* & -B^2LKP_2^* & 0 & 0 & 0 & 0 & 0 & 0 \\ 0 & -B^2LKA_1^* & -B^2LKA_5^* & B^3LKA_2^* & 0 & 0 & 0 & 0 & 0 & 0 \\ 0 & 0 & 0 & 0 & 0 & 0 & 0 & 0 & 0 & 0 \\ 0 & 0 & 0 & 0 & 0 & 0 & 0 & 0 & 0 & 0 \\ 0 & 0 & 0 & 0 & 0 & 0 & 0 & 0 & 0 & 0 \\ 0 & 0 & 0 & 0 & 0 & 0 & 0 & BLKH_1^* & BLKH_5^* & -B^2LKH_2^* \\ 0 & 0 & 0 & 0 & 0 & 0 & 0 & BLKP_5^* & BLKP_1^* & -B^2LKP_2^* \\ 0 & 0 & 0 & 0 & 0 & 0 & 0 & -B^2LKA_1^* & -B^2LKA_5^* & B^3LKA_2^* \\ 0 & 0 & 0 & 0 & 0 & 0 & 0 & 0 & 0 & 0 \\ 0 & 0 & 0 & 0 & 0 & 0 & 0 & 0 & 0 & 0 \end{bmatrix} \quad (4)$$

where B is the deck width; L is the element's length; K is the reduced frequency, $K=B\omega/U$, ω is the response angular frequency; H_i^* , A_i^* , P_i^* ($i=1\sim 6$) are the experiment determined flutter derivatives, which are the functions of the reduced frequency and the effective wind attack angle α_e due to the static wind action.

The modal analysis method is used herein to solve Eq. (3). For a dynamic system, the response can be separated into the spatial (natural mode) and time-dependent (generalized coordinate) components as

$$\{u(x, t)\} = [\phi] \{ \xi(t) \} \quad (5)$$

where $[\phi]$ is mode matrix obtained from the dynamic characteristics analysis on the deformed bridge structure under the static wind action; $\{ \xi(t) \}$ is the generalized coordinate vector, which can be assumed as a damped harmonic form and represented in the complex plane as:

$$\{ \xi(t) \} = \{ R \} \exp(\lambda t) \quad (6)$$

where $\{ R \}$ is the response amplitude vector, whose components reflect the participation of each mode in flutter; $\lambda = (\delta + i)\omega$; δ is the response logarithmic decrement; ω is the response angular frequency; $i = \sqrt{-1}$.

Substituting Eqs. (5) and (6) into Eq. (3), then pre-multiplying the transpose of the mode matrix $[\phi]$, and considering the orthogonality between modes and existence of a nontrivial solution, a

determinant can be yielded as

$$\left| [M^g] \left(\frac{U}{B} \right)^2 S^2 + [D^g] \left(\frac{U}{B} \right) S + [K^g] - \frac{1}{2} \rho U^2 \left[[A_s^g] + \frac{1}{B} [A_d^g] i K \right] \right| = 0 \quad (7)$$

where, $[M^g] = [\phi]^T [M] [\phi]$, $[D^g] = [\phi]^T [D] [\phi]$, $[K^g] = [\phi]^T [K(\mathbf{u})] [\phi]$ are the generalized mass, damping and stiffness matrices respectively; $[A_s^g] = [\phi]^T [A_s(k, \alpha_e)] [\phi]$, $[A_d^g] = [\phi]^T [A_d(k, \alpha_e)] [\phi]$ are the generalized aerodynamic stiffness and damping matrices; $S = k(\delta + i)$.

For a given wind speed U , Eq. (7) can be solved by the PK-F method (Namini 1992). The value S , which makes the determinant equal to zero, represents the actual response. The logarithmic decrement and the angular frequency of response can be computed as:

$$\delta = \frac{\text{Re}(S)}{\text{Im}(S)}, \quad \omega = \frac{U}{B} \text{Im}(S) \quad (8)$$

where Re and Im are the real and imaginary parts of a complex variable respectively.

Depending on the sign of the logarithmic decrement, the response can be defined to be: $\delta < 0$, stable; $\delta = 0$, neutrally stable; $\delta > 0$, unstable. The wind speed that produces the neutrally stable is termed as flutter speed U_f , with the corresponding flutter frequency ω_f .

3. Computer implementation

Based on the above method, a computer program of three-dimensional nonlinear flutter analysis NFAB is developed to analyze the flutter stability of long-span bridges. The computational flow can be summarized as follows:

- (1) Input the bridge finite element model, flutter derivatives and aerostatic coefficients etc.
- (2) Determine the equilibrium position under the dead load by three-dimensional geometric nonlinear analysis.
- (3) Calculate the current wind speed U_{cur} , starting with U_{low} and incrementing with U_{inc} .
- (4) Predicate the aerostatic equilibrium position under current wind speed by three-dimensional nonlinear aerostatic analysis, which is the initial state of the motions under the dynamic wind action.
- (5) Structural dynamic characteristics is analyzed on the deformed aerostatic equilibrium position by the subspace iteration method, and the modes are selected to participate in flutter analysis.
- (6) Calculate the effective wind attack angle according to the deformation obtained in step (4), the aerodynamic stiffness matrix and the aerodynamic damping matrix are recalculated to take into account the nonlinear and three-dimensional effects of the aerodynamic force. Using the changed dynamic characteristics obtained in step (5), the determinant is established and solved to predicate the response state.
- (7) Define the state of aerodynamic response according to the logarithmic decrement. If $\delta < 0$, aerodynamic instability does not happen, then return to step (3), and repeat steps (4)-(6) until the flutter critical condition is reached.

To verify the accuracy and efficiency of the above method and the program, a simple-supported beam of 300 meters is taken as example as shown in Fig. 2. In the aerodynamic stability analysis, flutter derivatives of the airfoil are used (Scanlan and Tomoko 1971). Structural damping ratio is assumed to be zero. Table 1 shows the modal frequencies and shapes of the beam under the dead

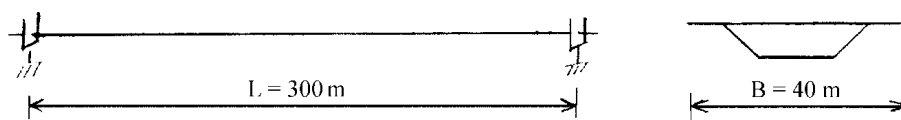


Fig. 2 The simple-supported beam and its cross section

Table 1 Modes participating in flutter

| Mode No. | Frequency (Hz) | Mode shape |
|----------|----------------|------------|
| 1 | 0.1788 | S-V |
| 2 | 0.5010 | S-T |
| 3 | 0.7153 | AS-V |
| 4 | 0.9897 | AS-T |

Note: S-symmetric, AS-asymmetric, V-vertical bending, T-torsion

Table 2 Comparison between the analytical results and accurate solutions

| Results | Critical wind speed (m/s) | Frequency (Hz) |
|--------------------|---------------------------|----------------|
| NFAB | 139.15 | 0.3789 |
| Accurate solutions | 139.9 | 0.3801 |

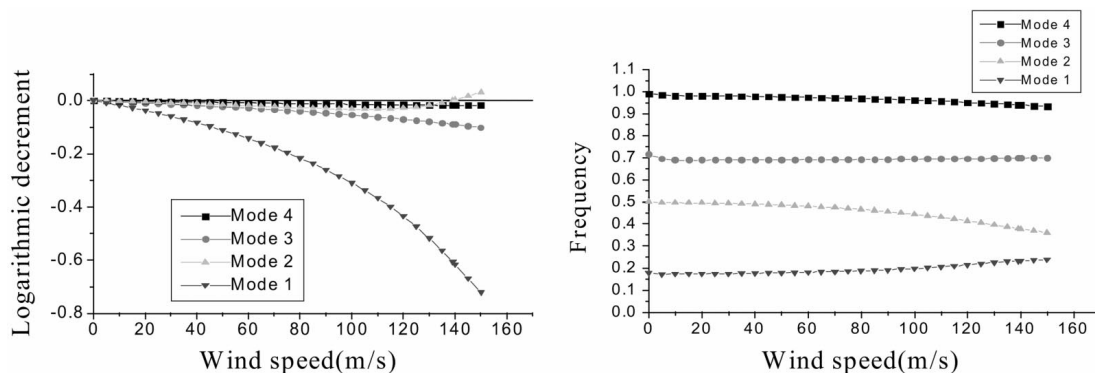


Fig. 3 Evolutions of the response logarithmic decrement and frequency with wind speed

load, which are selected to participate in flutter. The critical wind speed and frequency obtained analytically are compared to the accurate solutions as shown in Table 2. The evolutions of the logarithmic decrement and frequency of response with wind speed are plotted in Fig. 3.

As seen in Table 2, the results obtained analytically are just identical to the accurate solutions. Moreover as shown in Fig. 3, the dynamic response from the stable condition to the unstable condition can be clearly predicated. Therefore, it is demonstrated that the method and its computer program are both accurate and efficient to predicate the response under the dynamic wind action.

4. Parametric study

In order to comprehensively investigate the flutter stability of cable-stayed bridges, parametric analyses including the ratios of side span to main span and the tower's height to main span length, the tower's lateral configuration, and the subsidiary piers in side spans have been performed on the Jingsha bridge over the Yangtze River by the computer program NFAB.

The Jingsha bridge is a cable-stayed bridge with a center span of 500 m and two side spans of 200 m. The deck is a pre-stressed concrete structure of 27.0 m wide and 2.0 m high as shown in Fig. 4. The towers are H-shaped with 137-m height. There are two fan-shaped cable planes. A three-dimensional finite element model is established for the bridge as shown in Fig. 5, in which the towers and stiffening girders are modeled by three-dimensional geometric nonlinear beam elements, and the cables are modeled by three-dimensional geometric nonlinear truss element. The connections between the bridge components and the supports are properly modeled. The deck is idealized to a three-girder finite element model. The aerostatic coefficients and flutter derivatives under different wind attack angles are obtained from the section-model tests of the bridge (Song 1999). Structural damping is assumed as 1.0%. Since flutter stability of the bridge is the worst at the wind attack angle of -3° , the following analyses are all at this wind attack angle.

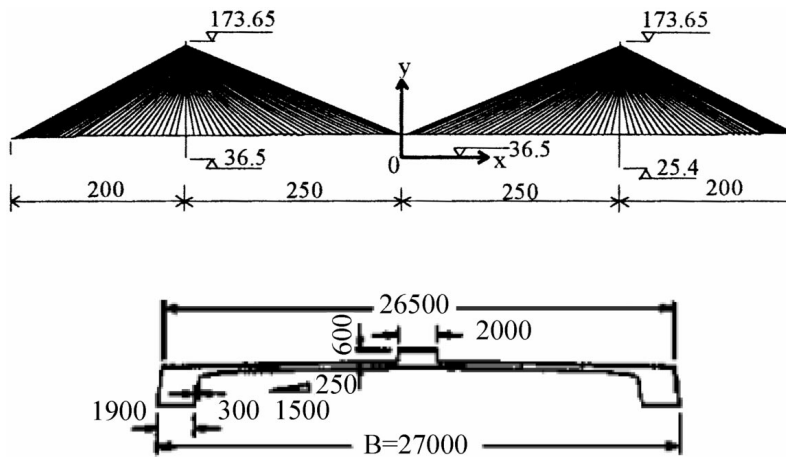


Fig. 4 General view of the Jingsha bridge over the Yangtze River

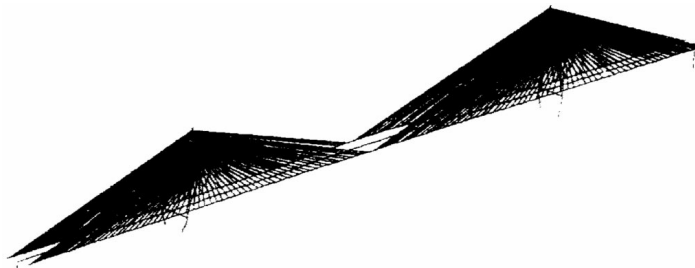


Fig. 5 Three-dimensional finite element model of the Jingsha bridge

It is to be noted that in the following analytical cases, the cross section areas of the stay cables are determined by the internal force under the dead and live loads with a safety factor of 2.5, and the sectional parameters of the stiffening girder including the cross section area, the bending and torsional moments of inertia, mass and mass moment of inertia per unit length etc are also determined on the basis of the supporting capacity of the stiffening girder.

4.1. Ratio of side span to main span

Statistics show that for cable-stayed bridges, the side span to main span ratio usually ranges from 1/3 to 1/2 (Yan 1996). To investigate the effect of the side span to main span ratio on flutter stability, the cases of side spans of 166 m, 200 m and 250 m (the side span to main span ratios are 0.33, 0.4 and 0.5 respectively) with the same center span are analyzed, the critical wind speeds of flutter stability obtained analytically are given in Table 3.

As the side span length increases, the critical wind speeds are slightly increased as seen in Table 3. The fact can be owed to the increase of the torsion to bending frequency ratio as given in Table 4. Meanwhile, the vertical stiffness of the bridge is greatly decreased with increasing of the side span length. Thus, the side span length can be determined according to the requirement of the bridge supporting capacity.

4.2. Ratio of the tower's height to main span length

It is to be noted that the tower's height discussed here is measured from the bridge deck level. Therefore, it is directly related to the inclined angles of the stay cables, which has important influence on the bridge stiffness and the dynamic characteristics. For cable-stayed bridges, the tower's height to main span length ratio usually ranges from 1/4 to 1/7, but are mostly close to 1/5 (Yan 1996). To investigate the effect of the tower's height on flutter stability, the cases as shown in Table 5 are analyzed, in which the other design parameters are all the same.

As can be seen in Table 5, the critical wind speed is achieved to the maximum value when the

Table 3 The critical wind speeds under different side span length

| Side span length (m) | 166 | 200 | 250 |
|---------------------------|------|------|------|
| Critical wind speed (m/s) | 73.4 | 74.5 | 76.8 |

Table 4 The modal frequencies and the torsion to bending frequency ratios

| Side span length (m) | 166 | 200 | 250 |
|----------------------|--------|--------|--------|
| 1-S-V(Hz) | 0.1925 | 0.1817 | 0.1406 |
| 1-S-T(Hz) | 0.3866 | 0.3911 | 0.3451 |
| Frequency ratio | 2.008 | 2.1524 | 2.535 |

Table 5 The critical wind speeds under the different tower's height to main span length ratios

| Ratios of the tower's height to main span length | 1/4.3 | 1/5 | 1/6 | 1/7 |
|--|-------|------|------|------|
| Critical wind speed (m/s) | 74.5 | 88.8 | 59.3 | 52.4 |

ratio of tower's height to main span length is assumed as 1/5. With the decrease of tower's height, the efficient supporting capacity of the stay cables is decreased, which results in the great decrease of structural stiffness and further the modal frequencies especially the torsional frequencies. The critical wind speeds are therefore significantly decreased. Besides the economics and supporting capacity of the bridge, to a great extent, the favorable tower's height can be determined by the wind-resistant requirement of the bridge.

4.3. The tower's lateral configuration

Generally, the arrangement of cable planes is parallel or inclined, which is directly related to the lateral configuration of the towers. In practice, the H-shaped, A-shaped and the reverse Y-shaped towers (above the deck level) are usually designed in modern cable-stayed bridges as shown in Fig. 6 (Yan 1996). To investigate the effect of the tower's lateral configuration on flutter stability, the bridges with different tower's lateral configurations are assumed and analyzed, in which the other design parameters are the same for all the cases. The modal frequencies and the critical wind speeds obtained analytically are both given in Table 6.

The frequencies of the 1st symmetric vertical bending modes are almost the same for all the cases, but the torsional frequencies in the other two cases are very close and both greater than that in the case of H-shaped towers designed for the bridge. As compared with the case of H-shaped towers, the torsional frequencies in the other two cases are greatly increased, and the amplitudes are

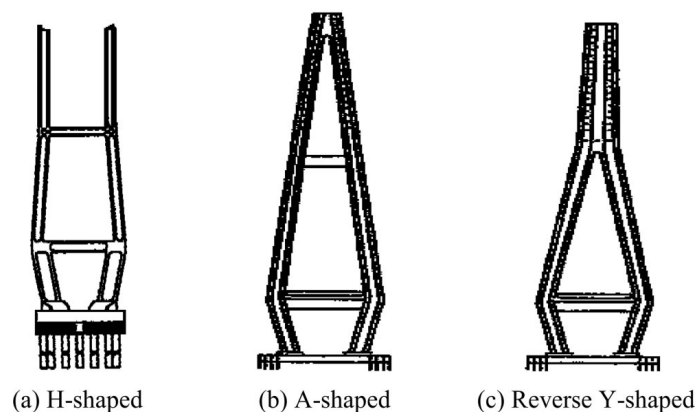


Fig. 6 The tower's lateral configurations

Table 6 The modal frequencies and the critical wind speeds under different tower's lateral configurations

| Tower's configuration | Frequency (Hz) | | Critical wind speed (m/s) |
|-----------------------|----------------|--------|---------------------------|
| | 1-S-V | 1-S-T | |
| H-shaped | 0.1817 | 0.3911 | 74.5 |
| A-shaped | 0.1818 | 0.5678 | 95.2 |
| Reverse Y-shaped | 0.1808 | 0.5712 | 96.2 |

Table 7 The modal frequencies and the critical wind speeds under different number of the subsidiary piers

| Number of the subsidiary piers | Frequency (Hz) | | Critical wind speed (m/s) |
|--------------------------------|----------------|--------|---------------------------|
| | 1-S-V | 1-S-T | |
| 0 | 0.1817 | 0.3911 | 74.5 |
| 1* | 0.2818 | 0.4298 | 74.5 |
| 2** | 0.2908 | 0.4348 | 74.9 |

Note: *the subsidiary is located 70 meters away from the abutment;

**Two subsidiary piers are located 70 m and 140 m away from the abutment respectively.

greater than 45%. With the significant increase of the torsional frequencies, the critical wind speeds are therefore significantly increased as shown in Table 6. Similarly, the critical wind speeds in the later two cases are increased by greater than 21 m/s. In fact, the arrangements of cable planes are inclined under the later two cases, whereas they are parallel in the case of H-shaped towers. Thus for cable-stayed bridges, the arrangement of inclined cable planes is helpful to improve the flutter stability of cable-stayed bridges, the A-shaped and the reverse Y-shaped towers are both aerodynamically favorable.

4.4. The subsidiary piers in side spans

For cable-stayed bridges, a few of subsidiary piers are usually installed in side spans (Yan 1996). As viewed from the dynamic characteristics, the subsidiary piers are helpful to increase the vertical bending stiffness. To investigate the effect of the subsidiary piers in side spans on the flutter stability, the cases under different number of the subsidiary piers in side spans are analyzed, the results are given in Table 7.

It is found from Table 7 that the subsidiary piers have almost no effect on the critical wind speeds. The fact can be attributed to the small variations of the torsional frequencies even though the vertical bending frequencies are greatly increased as the subsidiary piers are installed in side spans. Therefore, the subsidiary piers can be installed in side spans according to the requirement of the bridge supporting capacity.

5. Conclusions

Based on the method of nonlinear flutter analysis, parametric studies have been made for the Jingsha bridge over the Yangtze River, the effects of some design parameters on flutter stability are investigated. Some conclusions are summarized as follows:

- (1) The critical wind speed is slightly affected by the side span length. Thus, the side span length can be determined according to the requirement of the bridge supporting capacity.
- (2) The tower's height has important influence on the flutter stability of cable-stayed bridges. With the decrease of the tower's height, the critical wind speed will be greatly decreased. As the tower's height to main span length ratio is attained to 1/5, the critical wind speed will be achieved to the maximum value.
- (3) Flutter stability is remarkably improved by the arrangement of inclined cable planes. Therefore, it is suggested that the inclined cable planes should be designed for long-span and

especially super long-span cable-stayed bridges.

- (4) The A-shaped and the reverse Y-shaped towers are both aerodynamically favorable for cable-stayed bridges due to the inclined cable planes.
- (5) The subsidiary piers in side spans have almost no influence on flutter stability of cable-stayed bridges. Thus, the subsidiary piers can be installed in side spans according to the requirement of the bridge supporting capacity.

Acknowledgements

This project is supported by Zhejiang Provincial Science Foundation of China and China Postdoctoral Science Foundation, which are gratefully acknowledged.

References

- Agar, T.J. (1989), "Aerodynamic flutter analysis of suspension bridges by a modal technique", *Engrg. Struct.*, **11**, 75-82.
- Boonyapinyo, V., Yamada, H. and Miyata, T. (1994), "Wind-induced nonlinear lateral-torsional buckling of cable-stayed bridges", *J. Struct. Engrg.*, ASCE, **120**(2), 486-506.
- Chen, J., Jiang, J.J., Xiao, R.C. and Xiang, H.F. (2002), "Nonlinear aerostatic stability analysis of Jiangyin suspension bridge", *Engineering Structures*, **24**, 773-781.
- Ge, Y.J. and Tanaka, H. (2000), "Aerodynamic flutter analysis of cable-supported bridges by multi-mode and full-mode approaches", *J. Wind Engrg. Indust. Aerodyn.*, **86**, 125-153.
- Jain, A., Jones, N.P. and Scanlan, R.H. (1996), "Coupled aeroelastic and aerodynamic response analysis of long-span bridge", *J. Wind Engrg. Indust. Aerodyn.*, **60**, 69-80.
- Namini, A.H. (1992), "Finite element-based flutter analysis of cable-suspended bridge", *J. Struct. Engrg.*, ASCE, **118**(6), 1509-1526.
- Scanlan, R.H. and Jones, N.P. (1990), "Aeroelastic analysis of cable-stayed bridges", *J. Struct. Engrg.*, ASCE, **116**(2), 279-297.
- Scanlan, R.H. and Tomoko, J.J. (1971), "Airfoil and bridge deck flutter derivatives", *J. Eng. Mech. Div.* ASCE, **97**(6), 1717-1737.
- Song, J.Z. (1999), *Wind-resistant Research on the Jingsha bridge*. Res. Rep. of Tongji University, Shanghai.
- Tanaka, H., Yamamura, N. and Tatsumi, M. (1992), "Coupled mode flutter analysis using flutter derivatives", *J. Wind. Engrg. Ind. Aerodyn.*, **41-44**, 1279-1290.
- Yan, G.M. (1996), *Modern Cable-Stayed Bridges*, Southwest Jiaotong University Press.
- Zhang, X.J., Sun, B.N. and Xiang, H.F. (2002), "Nonlinear aerostatic and aerodynamic analysis of long-span suspension bridges considering wind-structure interactions", *J. Wind Engrg. Indust. Aerodyn.*, **90**(9), 1065-1080.
- Zhang, X.J., Chen, A.R. and Xiang, H.F. (2002), "Three-dimensional nonlinear flutter analysis of long-span suspension bridges", *China Civil Engineering Journal*, **35**(5), 42-46 (in Chinese).
- Zhang, X.J. (2000), "Three-dimensional nonlinear flutter analysis of long-span bridges", PhD thesis, Tongji University, Shanghai, China (in Chinese).